Al-Azhar Bulletin of Science

Volume 32 | Issue 2 Article 10

12-1-2021
Section: Chemistry

Synthesis, structural characterization, and catalytic reduction study of Co(II) complex towards toxic organic compounds; nitrophenol, and nitroaniline

Aml Saleh
Chemistry Department, Faculty of Science (Girl's), Al-Azhar University, Youssif Abbas St., Nasr-City, Cairo, Egypt., aml.mahmoud@azhar.edu.eg

Abeer Faheim
Chemistry Department, Faculty of Science (Girl's), Al-Azhar University, Youssif Abbas St., Nasr-City, Cairo, Egypt., afaheim@azhar.edu.eg

Omayma Mostafa
Chemistry Department, Faculty of Women for Arts, Science, and Education, Ain Shams University, Cairo, Egypt, omaymaahmed92@yahoo.com

Zeinab Abdelwahab
Chemistry Department, Faculty of Science (Girl's), Al-Azhar University, Youssif Abbas St., Nasr-City, Cairo, Egypt., zhabdelwahab@yahoo.com

Aida Salman
Chemistry Department, Faculty of Science (Girl's), Al-Azhar University, Youssif Abbas St., Nasr-City, Cairo, Egypt., aidasalman.5920@azhar.edu.eg

How to Cite This Article

Saleh, Aml; Faheim, Abeer; Mostafa, Omayma; Abdelwahab, Zeinab; and Salman, Aida (2021) "Synthesis, structural characterization, and catalytic reduction study of Co(II) complex towards toxic organic compounds; nitrophenol, and nitroaniline," *Al-Azhar Bulletin of Science*: Vol. 32: Iss. 2, Article 10.
DOI: https://doi.org/10.21608/absb.2021.94121.1135

Al-Azhar Bulletin of Science: Section A, Vol. 32, No. 2, (December) 2021, pp. 11-21
http://doi.10.21608/absb.2021.94121.1135

Al-Azhar Bulletin of Science: Section A

SYNTHESIS, STRUCTURAL CHARACTERIZATION, AND CATALYTIC REDUCTION STUDY OF Co(II) COMPLEX TOWARDS TOXIC ORGANIC COMPOUNDS; NITROPHENOL, AND NITROANILINE

Aml M. Saleh [a], Abeer A. Faheim [a], Omyma A. M. Ali [b], Zeinab H. Abd El – Wahab [a], and Aida A. Salman [a]

[a] Chemistry Department, Faculty of Science (Girl's), Al-Azhar University, Youssif Abbas St., Nasr-City, Cairo, Egypt, P.O. Box 11754

[b] Chemistry Department, Faculty of Women for Arts, Science, and Education, Ain Shams University, Cairo, Egypt

* Corresponding Author: aml.mahmoud@azhar.edu.eg

Received: 17 Sep 2021; Revised: 03 Nov 2021; Accepted: 15 Nov 2021; Published: 01 Dec 2021

ABSTRACT

Electrolysis (ED) is a modern technology for separating pollutants using membranes located in an electric field and has therefore been used in industrial wastewater treatment. The cornerstone of an ED cell is a stack of membranes whose planar plate is composed of cation (CM) and anion (AM) selective membranes. To investigate design requirements such as limiting current density (LCD), current efficiency and membrane resistance by laboratory experimental scale using an ED cell with electrodes, stainless steel 316 [cathode (-) and anode (+)],value of pH equal 6.8 and low voltage supply energy of 24.8 V is installed to remove about 100mg/L for each metal (Iron, Manganese, Nickel, Copper, Zinc, Lead, and Cadmium) ions out of solution of salts. The modified membranes and electrodes to upgrade its durability and conductivity, the recycle flow was 90 and 34 L/hr for concentrate and product, respectively, which are 25 and 9.4 ml/s and with consumed 7 to 11 kWh/m^3 for a continuous operation. For industrial wastewater; the results are obtained a best and encouraging specific with removal efficiency (up to 91.87%) during the 4 hr operating time. The result of removing heavy metal ions was 1.521, 0.96, 0.123, 1.41, 0.94, 0.12 and 0.097 mg/L as initial concentrated and after passing through ED cell became finial concentration 0.23, 0.11, 0.01, 0.22, 0.14, 0.02 and 0.014 with removal efficiency 84.88, 88.54, 91.87, 84.40, 85.11, 83.33 and 85.57% for heavy metal ions under study respectively. The next is being acted on large scale for long operating system.

Keywords: Industrial wastewater; Electrodialysis technology; Heavy metals; Anion membrane; Cation membrane.

1. INTRODUCTION

For all living organisms on earth, humans' activities, and the development, in addition to the urban, agricultural, and industrial objectives, water is an essential and valuable resource [1-3]. The high dissolving capacity of water for the different species, and the ease of water to form a suspension, to facilitate the transport of various pollutants into water sources and make the water pollution easily [4].

The literatures survey revealed that, the rapid industrialization, the advancements in technology, the economic development, a great number of variable service sectors, and other have an essential role in the various water resource pollutions. Moreover, different types of pollutants are released in the environment as heavy metal ions, dyes, phenols, biphenyls, pharmaceutical drugs, and pesticides. These toxic pollutants change the water quality, have significantly affected the ecosystem quality,

and causing harm to human health through the respiratory tracts as well as the food chain [5,6]. The chemical pollution of water is well-known as a major source of water quality damage, and represents a menace to the aquatic environment, with serious effects like acute and chronic toxicity in aquatic organisms, accumulation of pollutants in the ecosystem [7]. From the other hand, there are different physical, and chemical techniques were applied to treat the polluted water as chemical precipitation processes, degradation using biological agents, adsorption, and other. Some of them have several disadvantages as inconvenient, non-destructive, and insensitive methods for detecting pollutants, and so, their action is limited to the transfer of the pollutant species from the pollutant phase to another one that is also contaminated, then the pollutants still exist [8].

2. EXPERIMENTAL WORK

2.1. Materials and reagents

All chemical used in this work were of highest purity available. They include: silver nitrate ($AgNO_3$) and cobalt chloride hexahydrate ($CoCl_2.6H_2O$), (Merck or Aldrich); sulfadimidine (99% purity, Sigma); 3-acetylcoumarine, (Merk); *4*-Nitrophenol, *4*-Nitroaniline and organic solvents like ethyl alcohol, diethyl ether, DMF, DMSO and acetone (Sigma, Aldrich, Merk, Adwic); hydrochloric, nitric, and *sulfuric* acids were analytical grade and were used as supplied.

2.2. Synthesis of organic ligand

The organic ligand was synthesized through condensation reaction of an equimolar ratio of an ethanolic solution of 3-acetylcoumarine, and sulfadimidine under stirring at room temperature in presence of few drops of glacial acetic acid. After that, the mixture was refluxed for 6 hrs. with constant stirring on a water bath. The product thus formed on cooling was filtered, washed several times by ethanol then by ethyl ether and finally dried in vacuum desiccators over anhydrous $CaCl_2$.

2.3. Synthesis of cobalt (II) complex

Preparation of cobalt (II) complex was done by gradually addition of an aqueous solution of cobalt chloride hexahydrate (0.01M) to an ethanolic solution of the ligand, HL (0.01M) in presence of few drops of KOH solution under stirring at room temperature. After complete addition, the reaction mixture was refluxed for 4h with constant stirring on a water bath. During this period a precipitation of cobalt (II) complex has started. At the end, the precipitate was filtered off under the hot condition, washed with ethyl alcohol then diethyl ether and finally dried in vacuum desiccators over anhydrous $CaCl_2$.

2.4. Instrumentation

Elemental analysis of carbon, hydrogen, nitrogen and sulfur were performed using Perkin-Elmer CHN 2400 elemental analyzer. IR measurements (KBr pellets) were carried out on a Shimadzu 80 0 0 FT–IR spectrometer. The ^{1}H NMR spectra were recorded in DMSO–*d6* on a Bruker 500 MHz spectrophotometer using TMS as an internal reference. The UV-VIS spectra were measured on a Shimadzu UV-2600 spectrophotometer. The (TG - DTG) for compounds under study were recorded from ambient temperature to 1000 °C with a heating rate of 10 °C/min under a nitrogen atmosphere by shimaduz TG-50H and DSC-H50 thermal analyzer. The conductivity measurements were performed in DMSO at ambient temperature, by using Jenway 4010 conductivity meter. Magnetic measurements in the solid-state (Gouy method) were carried out on a Sherwood magnetic susceptibility balance. Mass spectrometry (70 eV, EI, Finni- gan MAT SSQ70 0 0 spectrometer).

2.5. Catalytic reduction of 4-nitro aromatic compounds

2.5.1. Catalytic reduction of 4-nitrophenol

In a clean flask containing 1mL of an aqueous solution of *4*-nitrophenol (*4*-NP) (1 mMol), add 10 mL of freshly prepared an aqueous solution of sodium boron hydride

($NaBH_4$) (50 mMol) with continuous stirring at room temperature. A rapid color change was observed from light yellow to bright yellow. After that, to this mixture, 0.01g of Co(II) complex was added as a catalyst and observe the color change of the reaction mixture, and also, the time taken for the experiment was noted. The decolorization of the mixture indicated the complete reduction of 4-NP (yellow colored solution) to 4-AP (colorless solution). A blank reaction was also performed in the absence of the catalyst [9,10].

2.5.2. Catalytic reduction of 4-nitroaniline

In a clean flask, 25 ml of an aqueous solution of 0.05 M $NaBH_4$ was mixed with 1 ml of an aqueous solution of 1 mM *4*-nitroaniline (4-NA), and 0.01gm of Co(II) complex as a catalyst. To study the catalytic efficiency of Co(II)complex, an aliquot amount of reaction mixture (3 mL) was taken, filter, and the progress of the reaction was determined by UV–Visible spectrophotometer for a period of time [11]**.**

3. RESULTS AND DISCUSSION

Considering the structural interesting of both 3-acetylcoumarine and sulfadimidine, their interaction is expected to produce a significance organic ligand for interested different applications. In this work, 3-acetylcoumarin was reacted successfully with sulfamethazine in a one-step condensation reaction to give a new ligand, HL as: Yellow solid, Mol. Formula $C_{23}H_{20}N_4O_4S$; yield=76.84%; M.P:168 ºC; Elemental anal. {Found (Calcd.)}: C, 61.50 (61.59); H, 4.12 (4.50); N, 13.00 (12.49); and S, 7.12 (7.13). This ligand possesses different strong donor sites; imine group (C=N), lactone carbonyl group (C=O), sulfonamide group (SO_2NH), and pyrimidine ring nitrogen. So, this ligand can act as a multidentate ligand as demonstrated by its structure, Fig. 1. Additionally, the ligand, HL is a key for further syntheses of Co(II) complex. The synthesized imine ligand, HL was reacted with Co(II) ion giving Co(II) complex as: Rose solid; Mol. Formula $[Co_2C_{23}H_{19}N_4O_4S\ (H_2O)\ Cl_3].2H_2O$; yield=75.8%; M.P > 360 ºC; Elemental anal. {Found (Calcd.)(%)}: C, 38.35 (38.06); H, 2.75 (2.64); N, 7.55 (7.72); S, 4.75 (4.41); Cl, 14.76 (14.65); Co(II), 15.90 (16.24); and 11.62 $\Omega^{-1}mol^{-1}\ cm^2$.

The structure of the synthesized ligand, and its Co(II) complex was elucidated utilizing the elemental analysis in addition to the spectroscopic study (IR, ^{1}H-NMR, mass, and UV–Vis), elemental analyses, molar conductance, effective magnetic moment, and thermal analysis (TGA / DTG). Moreover, catalytic potential of the Co(II) complex towards *4*-nitrophenol, and *4*-nitroaniline have been studied.

3.1. Elemental analyses

The formulation of the Schiff base (HL) ligand, and its Co(II) complex were confirmed by their elemental analysis. The metal to ligand ratio was found to be 2:1, and hence the Co(II) complex is a binuclear complex. This is achieved through estimation the C, H, N, S, Cl, and Co contents. The elemental analyses of the ligand, HL, and its Co(II) complex reveal a good agreement with the suggested molecular formula**.**

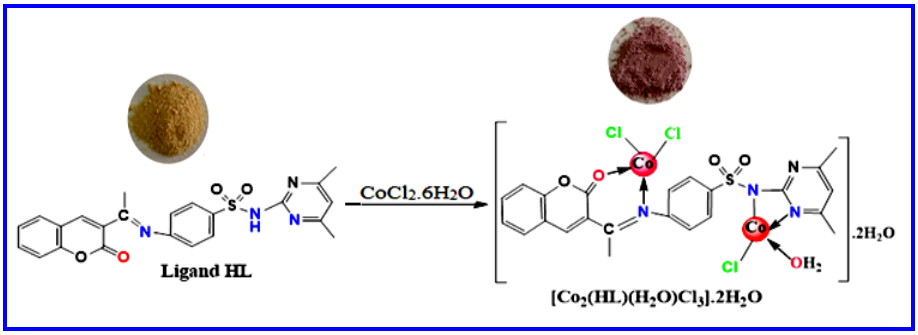

Fig. 1. Suggested structure of ligand HL and its Co(II) complex

3.2. Molar conductance measurements

The molar conductivity measurement for 1×10^{-2} M of Co(II) complex in DMSO at room temperature (2.42 $\Omega^{-1}mol^{-1}cm^{2}$) indicates its non-electrolytic nature[12].

3.3. Infrared spectra investigation

A careful comparison of the IR spectrum of the free ligand, HL with its Co(II) complex spectrum, Fig. 2 gives an indication about the binding sites in the ligand, HL that available for coordination with the Co(II) ion. In the infrared spectrum of the ligand, there are two main features. The first one is the disappearance of the peaks attributed to the amino group of sulfadimidine, and carbonyl group of acetyl moiety of acetylcoumarine with appearance of a new band at 1620 cm^{-1}. This band is due to imine group (C=N) as the main characteristic band confirming the condensation reaction, and supporting the formation of the proposed structure of the ligand, HL [13]. The second feature is the presence of two characteristic peaks in the infrared spectrum of ligand, HL at 1736, and 3426 cm^{-1}assigned to the characteristic vibrations of carbonyl υ(C=O), and amide υ(NH)groups of lactone fragment and sulfonamide moiety, respectively [14,15]. This is a more confirmation of the ligand formulation. The IR ligand spectrum displays two peaks at 1381 and 1142 cm^{-1}indicating the presence of $-SO_2NH-$ (symmetric and asymmetric vibrations) of sulfonamide moiety, respectively [16]. Other significant stretches vibrations assigned to υ(S-N), and υ(C-S) were observed in the IR ligand spectrum at 872, and 679 cm^{-1}, respectively [17,18]. Moreover, the peaks appearing in the region 1088 cm^{-1} attributed to pyrimidine ring [19].

By a careful examination of the recorded spectra of the synthesized Co(II) complex, the most notable change can be pointed out:

- IR spectrum of Co(II) complex shows a lower shift of the lactone υ(C=O), and imine υ(C=N) to 1636, and 1597 cm^{-1} compared with the free ligand (1736, and 1620 cm^{-1}), respectively. This shift indicates participation of the carbonyl lactone oxygen, and imine nitrogen in the complex formation [20,21]. Additionally, this coordination behavior of the ligand towards Co(II) ion is also proved by the appearance of the non-ligand bands of a medium intensity at 548, and 602 cm^{-1} due to υ(M–N), and υ(M–O), respectively [22].
- The υ(S–N) stretching vibration band that occur at 872 cm^{-1} in the free ligand shifted to a higher wave number 880 cm^{-1} confirming the coordination of Co(II) ion through the sulfonamido nitrogen atom [23].
- A notable change observed in Co(II) complex spectrum for the vibration of pyrimidine nucleus, ν(N=C) to a lower frequency (1080 cm^{-1}) with respect to the free ligand, (1088 cm^{-1}) indicating the involvement of N-heterocyclic atom in coordination with Co(II) ion [24].

3.4. ^{1}H-NMR spectroscopy

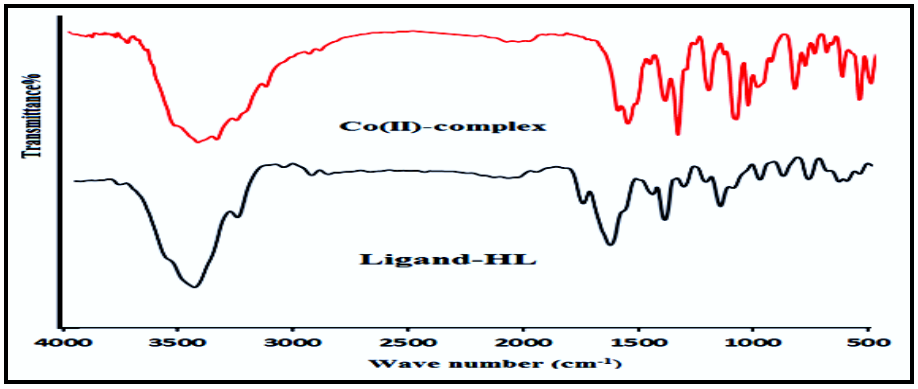

Fig. 2. IR spectra of the ligand HL and its Co(II) complex

The ^{1}H NMR spectrum of the ligand, HL was measured in (DMSO–d_6). The NMR data were reported in parts per million (ppm), and all exchangeable protons were determined by addition of D_2O. ^{1}H NMR spectrum of the free ligand, HL displayed SO_2NH proton as a singlet signal at δ 10.97 ppm (exchangeable with D_2O) [25]. The multiplet observed in the range of δ 6.53-7.66 ppm region belong to aromatic and heterocyclic protons [20]. Additionally, the methyl protons attached to the acetyl moiety was appeared as singlet at δ 2.493-2.544 ppm, while the methyl protons attached to the pyrimidine ring was observed as singlet at δ 2.24-2.51 ppm in ligand spectrum [26].

3.5. Mass spectral studies.

Further confirmations for the proposed structures for the studied ligand and its Co(II) complex were gained from their mass spectra data. The recorded mass spectra, Fig.3 showed the molecular ion peaks at m/z (intensity) 448.39 (73.96%), and 726.95 (22.44%)amu in agreement with the suggested molecular weights 448.49, and 725.73 amu for ligand, HL ($C_{23}H_{20}N_4O_4S$), and Co(II) complex {$[Co_2(HL)(H_2O)Cl_3].2H_2O$}, respectively. These determine molecular formula of the assigned ligand HL and its Co(II) complex are matched well with elemental analyses and thermogravimetric study.

3.6. Magnetic susceptibility data and electronic spectra

The magnetic behavior of the Co(II) complex was investigated via the molar magnetic susceptibility measurement in the solid state at room temperature. Such measurement used for the determination of the number of unpaired electrons, and geometrical structure [27]. The corrected magnetic moment value of Co(II) complex per metal ion using Pascal's constants, 5.39 BM indicating presence of three unpaired electrons, moreover this value is higher than the spin-only value (3.87) due to the orbital angular momentum contribution in a d^7-system [28].

The absorption electronic spectra of the free ligand, HL and its Co(II) complex were measured in DMF at room temperature from 200 to 800 nm. The free ligand spectrum showed two bands at 325 and 349 nm. The higher energy band is assigned to π–π* transitions of the phenyl, and the two heterocyclic rings; pyrimidine and coumarin in addition to C=N, C=O and S=O groups while the medium energy band is assigned ton–π*transitions for the electrons distributed on C=N, C=O, and S=O groups [29]. The spectrum of Co(II) complex indicates the appearance of a new peaks at higher wavelength; 430 and 530 nm may be assigned to ligand metal charge transfer, and d–d transitions; $^4A_2(F)\rightarrow{}^4T_1(P)$ transition, respectively. This is a positive evidence of

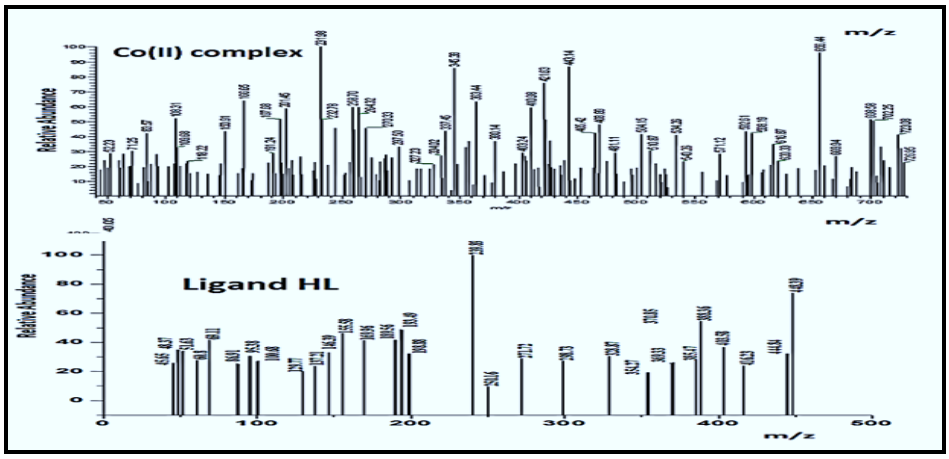

Fig. 3. Mass spectroscopy of ligand HL and its Co(II) complex

complex formation suggesting tetrahedral geometry [30].

3.7. Thermal properties study

Thermal behavior of the ligand, HL and its Co(II) complex has been studied through TGA-DTG analysis (Fig. 4). The temperature ranges, percentage mass losses, and the nature of each event of the decomposition reactions are given in Table 1 together with the decomposed and residual species. The thermal study explains that:

♦ The ligand, HL have a good thermal stability and its thermo gram demonstrates no weight loss was observed below 166°C indicating the absence of water in its structure. The first step of decomposition of ligand, HL at a temperature range of 166-350°C.

♦ Co(II) complex have hydrated water molecules where its decomposition starts at 35°C. Moreover, it exhibited five stages of weight loss in comparison to two stages of weight loss for its parent ligand.

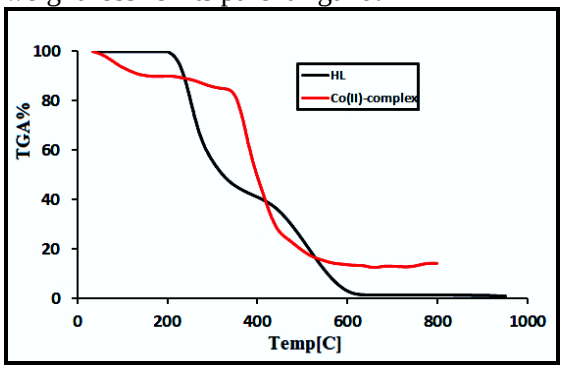

Fig. 4. TG-thermogram of the ligand HL and its Co(II) complex

To analyze the TGA curves and to get on the kinetic thermodynamic parameters for the decomposition stages, Coats-Redfern and Eyring equations [31] have been applied and the calculated data are listed in Table 2 and Fig. 5. According to the kinetic data obtained from TGA curves, the negative ΔH* values signifies that the decomposition processes are exothermic. The calculated ΔS* values were negative for all complexes. This suggests that the reactions take place slowly. The ΔG* values increase for the frequently decomposition steps due to increasing TΔS* values which surpassed ΔH* values [30].

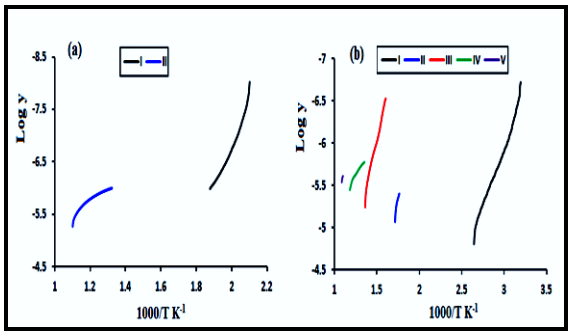

Fig. 5. Coats-Redfern plots of: (a) HL; (b) [Co-complex
$\log y = \log[\log\{W_\infty(W_\infty - W)^{-1}\}T^{-2}]$.

3.8. Evaluation of Co(II) complex as catalyst.

3.8.1. Catalytic reduction of *4*-nitrophenol

The catalytic activity of the prepared Co(II) complex was tested for the reduction of *4*-nitrophenol (*4*-NP) into its corresponding *4*-amino phenol (4-AP) using $NaBH_4$ as a reducing agent at room temperature. The study reveals that, in the absence of Co(II) complex, 4-NP does not get reduced. Co(II) complex took 90 min for reducing 4-NP solution as indicated via the decolorization of the mixture color [32].

3.8.2. Catalytic reduction of *4*-nitroaniline

Catalytic proficiency of Co(II) complex was examined by reducing *4*-NA (0.001 M) using $NaBH_4$ (0.05 M) and (0.01 gm) of catalyst at room temp. However, the reduction of *4*-nitroaniline to *4*-phenylenediamine (*4*-PDA) by borohydride without catalyst is quite slow. The catalytic activities of Co(II) complex for the *4*-NA reduction was determined by observing the color change of *4*-NA from yellow to faded, and observing the decrease of absorbance at 381 nm as the typical peak of *4*-NA. Presence of the *4*-PDA can further be confirmed with the appearance of the peak near 305 nm which are considered the distinctive peak for the *4*-PDA. The progress of catalytic reduction can be observed by measuring the decrease in absorbance with time as shown in Fig. 6. The percent reduction of *4*-NA is estimated. The percent reduction as a function

of time in the presence of the catalyst is shown in Table 3, and Fig .7.

$$\% \text{ Reduction} = [(C_0 - C_t) / C_0] \times 100$$

Where C_0 is the initial concentration of *4*-NP at time t equal to zero, and C_t is the concentration at different intervals of time (t) [33]. Moreover, the apparent reduction rate constant (k) can be determined by applying pseudo-first-order kinetics with respect to the concentration of *4*-NA [34]. Plotting of $Ln(A_0/A_t)$ versus time (t) (as shown in Fig. 8) allow to estimate apparent reduction rate constant (k) from slope of the linearly, and so, the value of $t._5$ is also calculated and listed in Table 4 [35]. Since k_{app} is referred to the mass of the catalyst used for the reaction, it is better to define the rate constant as specific rate constant (K′). K_{app} and (K′) are calculated for and listed in Table 4.

$$K' = k_{app}/m$$

Where m represents the catalyst mass used in g.

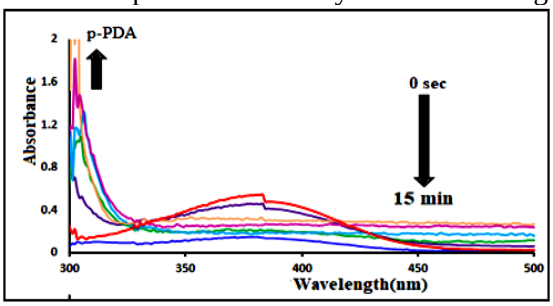

Fig. 6. UV–vis spectra of reduction of 4-NA without catalyst

and in the presence of Co(II) complex as catalyst.

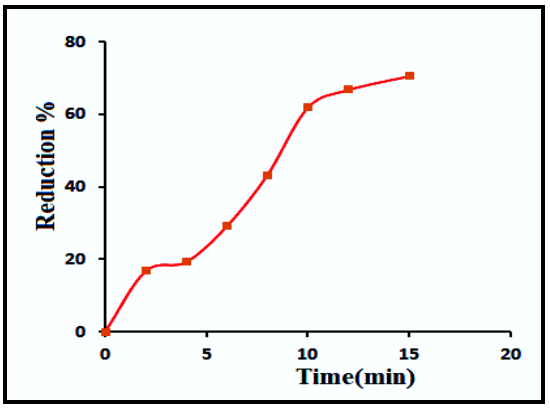

Fig. 7. The reduction of 4-NA in the presence of Co(II) complex.

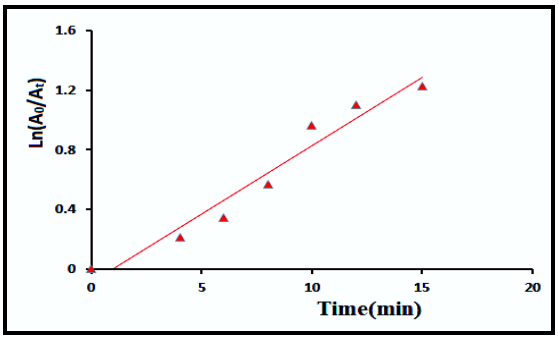

Fig. 8. Rate kinetics for reduction of 4-NA in the presence of Co(II)complex.

Furthermore, the turn over frequency (TOF) and the turnover number (TON) of catalyst were estimated as given in Table 4 [36]. Moreover, the apparent reduction rate constant (k) can be determined by applying pseudo-first-order kinetics with respect to the concentration

Table 1: Thermogravimetric data of ligand, HL and its Co(II) complex

Compound	Stage	Temp. range (°C)	DSC peak ˚C Endo↓ Exo↑	Heat mJ	Mass loss (%)		Evolved moiety	Residue (%) Found (Calcd.)
					Calcd	Found		
HL $C_{23}H_{20}N_4O_2S$	I	166-350	197 ↓ and 292 ↓	-218 and -138	62.48	62.24	SO_2, NO_2, N_2, $5C_2H_2$, C	$C_{12}H_{10}N$
	II	400-635			37.51	37.76	C_6H_5- C_6H_5	No residue
$[Co_2(L)(H_2O)Cl_3].2H_2O$ $[Co_2C_{23}H_{19}N_4O_4S(H_2O)Cl_3].2H_2O$	I	35-105	165 ↓; 296 ↓ and 372 ↓	-391, -24 and -335	6.20	6.39	2½ H_2O	$Co_2C_{23}H_{19}N_4O_4S(H_2O)_{½}Cl_3$
	II	235-310			3.44	3.79	½ H_2O, ½O_2	$Co_2C_{23}H_{19}N_4O_3SCl_3$
	III	350-460			58.38	58.56	2N_2, HCL, Cl_2, SO, 2CO, 6C_2H_2	$Co_2C_9H_6$
	IV	465-585			9.90	9.89	6C	$Co_2C_3H_6$
	V	635-665			0.83	0.83	3H_2	2Co+3C, 21.2(20.53)

of *4*-NA. To estimate k_{app}, we plotted $Ln(A_0/A_t)$ versus time (t) (as shown in Fig. 8), $t_{.5}$ is also calculated and listed in Table 4. Since k_{app} is related to the mass of catalyst used for the reaction, it is better to define the rate constant as specific rate constant (K′) K_{app} and (K′) are calculated for all catalysts and listed in Table 4. Also, we calculatedthe turn over frequency (TOF) and the turnover number (TON) of catalysts to determine the efficiency of the catalyst, Table 4 [37].

4. CONCLUSION

Here, an imine ligand incorporated sulfonamide, and coumarin moiety in addition to its corresponding Co(II) complex were prepared and elucidation of structures by different techniques. From the analytical, and spectral data, the ligand, HL acts as a multidente donor coordinating to Co(II) ion through NONO donor sites. The Co(II) complex is non-electrolytic in nature and has tetrahedral geometry. The thermal stability of the ligand, and its Co(II) complex has been studied, and the thermodynamic parameters were determined from the thermal data using Coats - Redfern method. The catalytic activity of the Co(II) complex was determined towards the reduction of toxic *4*-nitrophenol and *4*-nitroaniline. This study opens up more application possibilities of the metal complexes as catalysts in industrial applications.

ACKNOWLEDGMENT

The authors are grateful to the chemistry department, Science, Al-azhar university for providing spectral facilities.

Table 2: Thermodynamic data of the decomposition of the ligand, HL and its Co(II)complex

Compound	Steps	Decomposition Temp. ˚C	DTGA peak	A (min^{-1})	$\Delta H^{\#}$ (J/mol)	$\Delta S^{\#}$ (J/mol)	$\Delta G^{\#}$ (J/mol)	Ea (J/mol)	R^2
HL	I	166-350	290.39	$1.223x10^{11}$	-4264.695	-37.448	15545.302	136.585	0.97
	II	400-635	574.03	1.839	-6471.664	-239.729	181475.732	51.216	0.93
$[Co_2(L)(H_2O)Cl_3].2H_2O$	I	35-105	92.69	$4.48x10^{23}$	-3155.172	205.532	-86190.058	206.108	0.98
	II	235-310	293.96	$408.14\ x10^{5}$	-4423.036	-104.296	52314.027	103.044	0.92
	III	350-460	417.67	19325.81	-5395.384	-169.596	106368.266	87.496	0.99
	IV	465-585	529.13	0.395	-6389.893	-260.762	194918.079	33.147	0.97
	V	635-665	657.58	799.42	-7566.646	-198.879	175401.902	87.754	0.94

Table 3: the catalytic reduction of 4NA in the presence of Co(II)-complex as a catalyst.

Time(min)	0	2	4	6	8	10	12	15
Co(II)-complex R%	0	16.77	19.27	29.13	43.26	61.93	66.85	70.62

Table 4: The kinetic parameters calculated from catalytic reduction of 4NA in presenc of Co(II)-complex as catalyst

Compound under study	**K_{app} (min^{-1})**	**$t_{.5}$ (min)**	K′ **($min^{-1}gm^{-1}$)**	**TON* (molecules/g)**	**TOF* {molecules / (g.min)}**
Co(II)complex	0.092	7.562	9.164	0.054	0.0036

*TON is the number of substrate molecules that can convert into products using 1 g of catalyst, while TOF is calculated as TON / time.

REFERENCES

[1] Mohammadtaghi V, Shubo D, Giovanni C, Wei W, Pingping M, Dengchao L, Gang Y, Regeneration of chitosan-based adsorbents used in heavy metal adsorption: A review, J. Separation and Purification Technology. 2019; 224: 373–387.

[2] Hailan Y, Shujing Y, Zhuotong Z, Guangming Z, Xiaofei T, Rong X, Jiajia W, Biao S, Li D, Meng Q, Yuanyuan Y, Fuhang X, Utilization of biochar for resource recovery from water: A review, Chemical Engineering Journal. 2020; 397: 125502.

[3] Ertugrul E, Maria H, Osman G, Mucahit S, Ali Y, New construction materials synthesized from water treatment sludge and fired clay brick wastes, J. Building Engineering. 2021; 42: 102471.

[4] Sasireka V, Anurag R, Senthilarasu S, Tapas KM, A Review on Heavy Metal Ions and Containing Dyes Removal Through Graphene Oxide-Based Adsorption Strategies for Textile Wastewater Treatment, J. Chem. Rec. 2021; 21: 1–42.

[5] Sumei L, Saisai S, Sha C, Hanbing L, Ziyi L, Yixuan L, Jiaying F, Linhua X, Jianrong L, Photocatalytic degradation of hazardous organic pollutants in water by Fe-MOFs and their composites: A review, J. Environmental Chemical Engineering. 2021; 9: 105967.

[6] Mu J, Yang J, Zhang D, Jia Q, Progress in Preparation of Metal Nanoclusters and Their Application in Detection of Environmental Pollutants, chinese journal of analytical chemistry. 2021; 49: 319–329.

[7] Kim O, Is the objective of the Water Framework Directive to deal with pollutant emissions at source coherently implemented by the EU's substance-specific legal acts? A comparison of the environmental risk control of pharmaceutical legislation with the REACH-, Biocidal Products- and Plant Protection Products Regulation, J. Sustainable Chemistry and Pharmacy. 2021; 20: 100386.

[8] A. Cabrera, C. Torresa S. Marchettib and S. Stewart, Degradation of methylene blue dye under dark and visible light conditions in presence of hybrid composites of nanostructured MgFe2O4 ferrites and oxygenated organic compounds, J. Environmental Chemical Engineering, 2020; 8: 104274.

[9] Shamim AH, Hu SH, Mohammad Y, Kang HP, Silver nanoparticles deposited on metal tungsten bronze as a reusable catalyst for the highly efficient catalytic hydrogenation/reduction of 4-nitrophenol, J. Catalysis Communications, 2020; 141: 106011.

[10] Ravi K, Ranjana G, Synthesis of nanocrystallineCuO–ZnO mixed metal oxide powder by a homogeneous precipitation method, J. Ceramics International, 2014; 40: 10919–10926.

[11] Zimin L, Jinsong D, Xingxing J, Pengfei L, Xuefeng J, Jiang Y, Polyurethane/Keratin/AgNPsnanofibrous mats as catalyst support for 4-nitroaniline reduction, J. Materials Letters, 2019; 237: 9–13.

[12] Liu. Y, Yang. L, Yin. D, Dang. Y, Yang. L, Zou.Q and Li. J, Solvent-free synthesis, characterization, biological activity of Schiff bases and their metal (II) complexes derived from ferrocenylchalcone, J. Organomet. Chem. 2019; 899:120903-120909.

[13] Dara MA, Hashim JA, Synthesis of new ß-lactam- N-(thiazol-2-yl) benzene sulfonamide hybrids: Their in vitro antimicrobial and in silico molecular docking studies, J. Mol. Struct.2020; 1222: 128904.

[14] Abou-Hussein. A.A, Wolfgang L, Synthesis, spectroscopic studies and inhibitory activity against bactria and fungi of acyclic and macrocyclic transition metal complexes containing a triaminecoumarine Schiff base ligand, J. SpectrochimicaActa Part A: Molecular and Biomolecular Spectroscopy, 2015; 141: 223–232.

[15] Lian W, Lu L, Xia W, Ming-Lin W, Jin-Ming L, Ru-Song Z, Spherical mesoporous covalent organic framework as a solid-phase extraction adsorbent for the ultrasensitive determination of sulfonamides in food and water samples by liquid chromatography-tandem mass spectrometry, J. Chromatography A, 2020; 1625: 461275.

[16] Syed AT, Muhammad A, Mahmood A, Muhammad I, Riaz H, Mehwish S, Muhammad Y, Muhammad M, Levofloxacin and sulfa drugs linked via Schiffbases: Exploring their urease inhibition, enzyme kinetics and in silicostudies, J. Molecular Structure, 2021; 1235: 130226.

[17] Diego M. G, Fernando FS, G.A. Echeverría, Oscar EP, Hiram P, Aida A, A detailed exploration of intermolecular interactions in 4-(4 dimethylaminobenzylideneamino)-N-(5-methyl-3-isoxazolyl) benzenesulfonamide and related Schiff bases: Crystal structure, spectral studies, DFT methods, Pixel energies and Hirshfeld surface analysis, J. SpectrochimicaActa Part A: Molecular and Biomolecular Spectroscopy, 2017; 185: 286–297.

[18] Ahmed AM, Molecular structure and spectroscopic properties of novel manganese(II)

complex with sulfamethazine drug, J. Molecular Structure, 2013; 1035: 114–123.

[19] Neelam M, Priyanka D, Prabhakar KV, Anurag K, Design, synthesis, and biological evaluation of thiourea and guanidine derivatives of pyrimidine-6-carboxylate, J. Res ChemIntermed, 2015; 41: 7981–7993.

[20] Saliha A, Ümmühan OO, Sevki A, Hamit A, Esra B, Kerem K, Synthesis, spectroscopic characterizations, carbonic anhydrase II inhibitory activity, anticancer activity and docking studies of new Schiffbases of sulfa drugs, J. Molecular Structure, 2021; 1223: 128911.

[21] Sangamesh AP, Shrishila NU, Ajaykumar DK, Vinod HN, Prema SB, Co(II), Ni(II) and Cu(II) complexes with coumarin-8-yl Schiff-bases: Spectroscopic, in vitro antimicrobial, DNA cleavage and fluorescence studies, J. SpectrochimicaActa Part A, 2011; 79: 1128–1136.

[22] Ismail A, Marwa GE, Nashwa M, Novel Synthesized BenzesulfonamideNanosized Complexes; Spectral Characterization, Molecular Docking, Molecular Modeling and Analytical Application, J. Inorg. Organomet. Polym. Mat., 2019; 29: 876–892.

[23] Peter AA, Gabriel AK, Paul O, Madeleine H, James R, Cobalt(II) complexes of the antibiotic sulfadiazine, the X-ray single crystal structure of [Co(C10H9N4O2S)2(CH3OH)2], J. InorganicaChimicaActa, 2006; 359: 3111–3116.

[24] Maram TB, Reem MA, Mohamed RS, Laila HA, Synthesis, structural characterization, DFT calculations, biological investigation, molecular docking and DNA binding of Co(II), Ni(II) and Cu(II) nanosized Schiff base complexes bearing pyrimidine moiety, J. Mol. Struct. 2019; 1183: 298-312.

[25] Imane H, Mouna S, Fadila B, Belkacem B, Mhamed B, Hocine M, Sofiane B, A new complex of Zinc (II) with sulfamethoxazole ligand: Synthesis, crystal structure, Hirshfeld surface analysis, thermal properties, DFT calculations and antibacterial/antifungal activities, J. Molecular Structure, 2021; 1244: 130903.

[26] Zahid HC, Moulay HY, Aliasghar J, Taibi BH, Identification of antibacterial and antifungal pharmacophore sites for potent bacteria and fungi inhibition: Indolenyl sulfonamide derivatives, European journal of Medicinal Chemistry, 2010; 45: 1189-1199.

[27] Alizadeh. A, Mohammadi. R, Bayat. F and Zhu. L, Proton transfer process in synthesis of 3-acetyl-4-(substituted ethylenyl) coumarins and chromeno[3,4-c]pyridines, J. Tetrahedron 2018; 74: 2085-2091.

[28] Jayakumar. S, Mahendiran. D, Selvan. D, Rahiman. A, Bis(imidazol-1-yl) methane-based heteroscorpionate metal(II) complexes: Theoretical, antimicrobial, antioxidant, in vitro cytotoxicity and c-Met tyrosine kinase studies, J. Molecular Structure, 2019; 1196: 567-577.

[29] Zeinab HA, Complexation of 4-amino-1,3 dimethyl-2,6 pyrimidine-dione derivatives with cobalt(II) and nickel(II) ions: synthesis, spectral, thermal and antimicrobial studies, J. Coordination Chemistry, 2008; 61: 1696–1709.

[30] Abeer AF, Safaa NA, Zeinab HA, Synthesis and characterization of binary and ternary complexes of Co(II), Ni(II), Cu(II) and Zn(II) ions based on 4-aminotoluene-3-sulfonic acid, J. Spectrochim. Acta, Part A: Mol. Biomol. Spectrosc., 2013; 105: 109–124.

[31] Ayman AA, Hemmat AE, Spectral, electrochemical, thermal, DNA binding ability, antioxidant and antibacterial studies of novel Ru(III) Schiff base complexes, J. Spectrochim. Acta, Part A: Mol. Biomol. Spectrosc. 2014; 124: 404–415.

[32] Anantharamaiah. P.N, Manasa. K.S, Sunil. K.Y.C, Fabrication of magnetically recoverable and reusable MgFe2O4/Ag3PO4 composite for catalytic reduction of 4-Nitrophenol, J. Solid State Sciences 2020; 106: 106302.

[33] Yoki Y, Dewangga OBA, Zulda AZ, SiO2/NiFe2O4 nanocomposites: Synthesis, characterization and their catalytic activity for 4-nitroaniline reduction, J. Mater. Chem. Phys. 2021; 261: 124243-124251.

[34] Madhusudan KM, Dipanjan S, Suraj K, Himani K, Amita P, N, S doped carbon dots—Plasmonic Au nanocomposites for visible light photocatalytic reduction of nitroaromatics, J. Mater. Res., 2018; 33: 3907-3616.

[35] Tushar KD, Mussel‐inspired Ag/poly(norepinephrine)/MnO2 heterogeneous nanocatalyst for efficient reduction of 4‐nitrophenol and 4‐nitroaniline: an alternative approach, J. Res. Chem. Intermed., 2020; 46: 3629–3650.

[36] Sachin RT, Balu T, Bhaskar SM, Nageshwar DK, Kinetic investigation for the catalytic reduction of nitrophenol using ionic liquid stabilized gold nanoparticles, J. RSC. Adv. 2018; 8: 38384-38391.

[37] Jiangyong L, Jinxing L, Rongfei Y, Xiaodong Y, Lixia W, Panming J, Versatile bifunctional nitrogen-doped porous carbon derived from biomass in catalytic reduction of 4-nitrophenol and oxidation of styrene Chinese, J. Catal. 41 (2020) 1217–1229.

تحضير وتوصيف تركيبى والاختزال الحفزي تجاه المركبات العضوية السامة ؛ نيترو فينول ونيترو أنيلين

أمل محمود صالح [1], عبير احمد فهيم [1], أميمية على مصطفى [2], زينب حلمى عبدالوهاب [1], عايده عبدالعال سالمان [1]

[1] قسم الكيمياء- كلية العلوم بنات- جامعة الازهربالقاهرة

[2] قسم الكيمياء-كلية البنات للأداب والعلوم والتربية-جامعة عين شمس بالقاهرة

الملخص:

يوضح هذا العمل تحضير متراكب الكوبلت من الليجاندالمشتق من السلفوناميد و الكومارين.وقد تم دراسة المركبات عن طريق جهاز التحليل العنصرى ,الأجهزة الطيفية (الأشعة تحت الحمراء، الأشعة فوق البنفسجية، طيف الكتلة وطيف الرنين النووى المغناطيسى) وكذلك أجهزة قياسات الخواص الحرارية، المغناطيسية والإلكتروليتية، درجة الإنصهار وقد تم إستنتاج طرق الترابط بين ايون الكوبلت وعامل التراكب العضوى حيث اتضح أن متراكب الكوبلت يتكون بنسبة جزيئية (2:1) (عامل التراكب العضوى : أيون الفلز). وكذلك تم دراسة قدرة متراكب الكوبلت كعامل مساعد على اختزال النيترو فينول ، والنيتروانلين في وجود $NaBH_4$ كعامل مختزل في درجة حرارة الغرفة في محاولات للتطبيقات الصناعية ، لا سيما في إزالة الملوثات العضوية العطرية.